C. R. Physique 13 (2012) 440–453

Contents lists available at SciVerse ScienceDirect

Comptes Rendus Physique

www.sciencedirect.com

Advances in nano-electromechanical systems

Quantum dynamics of a mechanical resonator driven by a cavity

Dynamique quantique d'un résonateur mécanique forcé par une cavité

Andrew D. Armour *, Denzil A. Rodrigues

School of Physics and Astronomy, University of Nottingham, Nottingham NG7 2RD, UK

ARTICLE INFO

Article history:
Available online 23 April 2012

Keywords:
Quantum dynamics
Mechanical resonator
Optomechanical systems

Mots-clés :
Dynamique quantique
Résonateur mécanique
Systèmes optomécaniques

ABSTRACT

We explore the quantum dynamics of a mechanical resonator whose position is coupled to the frequency of an optical (or microwave) cavity mode. When the cavity is driven at a frequency above resonance the mechanical resonator can gain energy and for sufficiently strong coupling this results in limit-cycle oscillations. Using a truncated Wigner function approach, which captures the zero-point fluctuations in the system, we develop an approximate analytic treatment of the resonator dynamics in the limit-cycle regime. We find that the limit-cycle oscillations produced by the cavity are associated with rather low levels of energy fluctuations in the resonator. Compared to a resonator at the same temperature which is driven by a pure harmonic drive to a given average energy, the cavity-driven oscillations can have much lower energy fluctuations. Furthermore, at sufficiently low temperatures, the cavity can drive the resonator into a non-classical state which is number-squeezed.

RÉSUMÉ

Nous explorons la dynamique quantique d'un résonateur mécanique dont la position est couplée à la fréquence d'un mode optique (ou micro-onde) de cavité. Quand la cavité est forcée à une fréquence au-dessus de la résonance, le résonateur mécanique peut gagner de l'énergie et, pour un couplage suffisamment fort, ceci a comme conséquence des oscillations de cycle limite. En utilisant une approche de fonctions de Wigner tronquées, qui rend compte des fluctuations de point zéro dans le système, nous développons un traitement analytique approximatif de la dynamique du résonateur dans le régime de cycle limite. Nous constatons que les oscillations de cycle limite produites par la cavité sont associées à des niveaux des fluctuations d'énergie dans le résonateur plutôt bas. Comparé à un résonateur à la même température qui est forcé par un signal harmonique pur à une énergie moyenne donnée, les oscillations forcées par la cavité peuvent avoir des fluctuations d'énergie bien inférieures. En outre, aux températures suffisamment basses, la cavité peut forcer le résonateur dans un état non-classique.

* Corresponding author.
E-mail address: andrew.armour@nottingham.ac.uk (A.D. Armour).

1631-0705/$ – see front matter
http://dx.doi.org/10.1016/j.crhy.2012.03.006

1. Introduction

Optomechanical systems consisting of an optical (or microwave) cavity in which one of the modes couples strongly to the center of mass motion of a mechanical resonator [1–3] are a subject of intense current interest. Over the last few years there has been rapid progress in experiments and these devices now seem ideal vehicles for exploring quantum behavior in micromechanical resonators [4–6].

In a typical set-up an optical cavity is formed with one fixed mirror and a second one mounted on a micromechanical resonator (e.g. in the form of a cantilever). When the cavity is driven by a laser which is close to one its mode frequencies photons build up in the cavity, but motion of the mechanical resonator (which has a much lower frequency than the cavity modes) changes the length of the cavity; the resulting change in the mode frequencies leads in turn to a change in the number of photons in the cavity [1–3]. The response of the cavity occupation to the motion of the mechanical oscillator provides a very sensitive way of monitoring the latter's motion [7]. However, there is more to the dynamics of the system as the radiation pressure from the photons leads to a back-action force on the mechanical resonator. This back-action from the cavity is undesirable in the context of measurement, but the coupled dynamics that it leads to can be exploited very effectively to control the state of the mechanical resonator.

The overall result of the back-action on the resonator dynamics depends strongly on the choice of the frequency for the laser used to drive the cavity. For drive frequencies below the cavity mode frequency (red detuning) the cavity tends to absorb energy from the mechanical resonator. In contrast, when the drive laser is above the cavity frequency (blue detuning) the mechanical resonator absorbs energy from the drive via the cavity.

In the red-detuned regime the main effect of the cavity back-action on the resonator is to damp the mechanical motion. The fluctuations associated with this damping arise from quantum fluctuations in the cavity and are very small (provided, for a microwave cavity, it is at cryogenic temperatures). Because the system is far from equilibrium, the fluctuation–dissipation theorem is in a sense subverted and although the overall effect of the cavity on the resonator in this regime is like an effective thermal bath, it is one which has a very low effective temperature [8–11]. Thus coupling a mechanical resonator to a cavity driven at a frequency below resonance provides a way of cooling it, an effect which is closely related to the laser cooling of trapped ions [8]. A series of recent experiments with optomechanical systems [12–16], and analogous devices in which the cavity is realized in the microwave regime [17,18], have demonstrated that this method can be very effective and recently it has been used to cool a mechanical resonator almost to its groundstate [18,16]. These experiments clearly set the stage for further developments in which the quantum nature of micromechanical systems can be probed and manipulated [5,6].

In the blue-detuned regime the dynamics is non-linear and a complex range of behaviors can occur, much of which has already been revealed in experiments [19–21]. For sufficiently strong optomechanical coupling and sufficiently weak mechanical damping, the energy pumped into the mechanical resonator can lead to self-sustained limit-cycle oscillations [19–24]. At stronger couplings, the system becomes bistable before eventually becoming multistable and then chaotic [19]. Most work has focussed on the classical dynamics in this regime, although recent investigations have also begun to explore the quantum behavior [25–28]. Because the self-sustained oscillations of the mechanical system occur via pumping which is mediated by the coherent coupling to the cavity, it is natural to think of the system in terms of the paradigms of laser physics [29,30].

Here we develop an approximate analytic treatment based on a truncated Wigner function approach that provides a description of the quantum dynamics of a cavity-resonator system. We use this approach to investigate the behavior of the system in the blue-detuned regime, focussing in particular on the limit-cycle oscillations. We find that the fluctuations in the amplitude of the limit-cycle oscillations are surprisingly small. In the highly idealized case of negligible temperature we find that the energy fluctuations of the oscillator can be reduced below those of a coherent state resulting in a non-classical number-squeezed state [30]. In the presence of thermal noise, the fluctuations in the energy of the cavity-driven resonator can be strongly suppressed compared to those of a resonator at the same temperature which is driven to the same average energy by a pure harmonic excitation. This behavior is linked to the low noise associated with the photons in the cavity. Just as the low-noise properties of the cavity lead to cooling of the mechanical resonator in the red-detuned regime, we find that the cavity tends to suppress fluctuations in the energy of the resonator when it undergoes limit-cycle oscillations in the blue-detuned regime. The work presented here expands and develops our previous publication on this topic [27].

This article is organized as follows. In Section 2 we introduce our model for the cavity-resonator system and describe how its dissipative dynamics can be described by a partial differential equation for a Wigner function. Then in Section 3 we formulate an effective stochastic description of the resonator dynamics which is valid in the regime where the amplitude of the resonator changes much more slowly than that of the cavity and obtain an approximate probability distribution for the energy of the resonator. We consider the case of red-detuned laser driving in Section 4, where cooling of the mechanical resonator occurs, and show that in this regime the usual expressions for the back-action damping and effective occupation number are recovered from our approximate probability distribution. In Section 5 we examine the dynamics in the blue-detuned regime, exploring the properties of the limit-cycle oscillations which the resonator undergoes and the associated dynamical transitions. We compare the predictions of our approximate analytic description with those of a numerical treatment and investigate the behavior of the fluctuations in the resonator energy at finite temperature. Finally, we present our conclusions in Section 6, and discuss promising future directions for research in this area.

2. Cavity-resonator model

We consider the standard set-up of an optical cavity in which one of the mirrors is mounted on a mechanical resonator. Including a laser drive applied to the cavity, the Hamiltonian (in a frame rotating at the cavity frequency) takes the form [8,9,11,25],

$$H = -\hbar\left[\Delta + \frac{g}{2}\left(b + b^\dagger\right)\right]a^\dagger a + \hbar\omega_m b^\dagger b + \hbar\Omega\left(a + a^\dagger\right) \tag{1}$$

where g is the strength of the optomechanical coupling, a and b are cavity and resonator lowering operators respectively, ω_m is the mechanical frequency and Ω parameterizes the strength of the laser drive. The cavity is driven at a frequency ω_d which is detuned from the cavity frequency ω_c ($\gg \omega_m$), by $\Delta = \omega_d - \omega_c$.

We will focus on the case where the coupling between the optical and mechanical degrees of freedom is weak, in the sense that it is much lower than the mechanical frequency, $g \ll 2\omega_m$, an assumption which allows us to make important approximations. However, it is worth noting that the Hamiltonian of the undriven system can be diagonalized exactly [4] and has eigenvalues $E_{n,m} = \hbar\omega_c n - \hbar g^2/(4\omega_m)n^2 + \hbar\omega_m m$, which provides an alternative starting point for calculations which focus on the very strong coupling regime, $g \sim \omega_m$ [31,32].

Assuming weak optomechanical coupling we can include the effects of the (weak) interactions with the surroundings of both the optical mode and mechanical resonator to a good approximation by simply using the standard Born–Markov descriptions that would apply in the limit of zero coupling. Thus the evolution of the system is described by the master equation [25],

$$\dot\rho = -\frac{i}{\hbar}[H, \rho] + \mathcal{L}_m\rho + \mathcal{L}_c\rho \tag{2}$$

where the interaction of the mechanical resonator to its thermalized surroundings at temperature T is described by the quantum optical Liouvillian [30],

$$\mathcal{L}_m\rho = -\frac{\gamma_m}{2}(\bar n + 1)\left(b^\dagger b\rho + \rho b^\dagger b - 2b\rho b^\dagger\right) - \frac{\gamma_m}{2}\bar n\left(bb^\dagger\rho + \rho bb^\dagger - 2b^\dagger\rho b\right)$$

where γ_m is the mechanical damping rate and $\bar n = [\exp(\hbar\omega_m/k_{\mathrm B}T) - 1]^{-1}$ is the average occupation number of the oscillator when in equilibrium at temperature T. The cavity dissipation is described by

$$\mathcal{L}_c\rho = -\gamma_c\left(a^\dagger a\rho + \rho a^\dagger a - 2a\rho a^\dagger\right)/2 \tag{3}$$

with γ_c the decay rate and since the optical frequency is much larger than the mechanical one, we can assume $\hbar\omega_c \gg k_{\mathrm B}T$, so that in this case thermal fluctuations can be neglected.

We proceed by carrying out a Wigner transformation of the master equation, which introduces the complex variables α and β for the phase space of the cavity and resonator respectively [30]. The Wigner function for the cavity-resonator system is

$$W(\alpha,\beta) = \left(\frac{1}{\pi^2}\right)^2 \int \mathrm{d}^2\eta_a \int \mathrm{d}^2\eta_b\, \mathrm{e}^{\eta_a^*\alpha - \eta_a\alpha^*}\mathrm{e}^{\eta_b^*\beta - \eta_b\beta^*} \times \mathrm{Tr}\left[\rho \mathrm{e}^{\eta_a a^\dagger - \eta_a^* a}\mathrm{e}^{\eta_b b^\dagger - \eta_b^* b}\right] \tag{4}$$

where α and β are the phase space variables for the cavity and resonator respectively. The Wigner-transformed master equation takes the form,

$$\begin{aligned}\frac{\partial W}{\partial t} = {} & -i\omega_m\left(\beta^*\frac{\partial}{\partial\beta^*} - \beta\frac{\partial}{\partial\beta}\right)W + i\Delta\left(\alpha^*\frac{\partial}{\partial\alpha^*} - \alpha\frac{\partial}{\partial\alpha}\right)W - i\Omega\left(\frac{\partial}{\partial\alpha^*} + \frac{\partial}{\partial\alpha}\right)W \\ & + i\frac{g}{2}(\beta+\beta^*)\left(\alpha^*\frac{\partial}{\partial\alpha^*} - \alpha\frac{\partial}{\partial\alpha}\right)W + i\frac{g}{2}\left(\frac{\partial}{\partial\beta^*} - \frac{\partial}{\partial\beta}\right)\left(\alpha^*\alpha - \frac{1}{2} - \frac{1}{4}\frac{\partial^2}{\partial\alpha^*\partial\alpha}\right)W \\ & + \frac{\gamma_m}{2}\left(\frac{\partial(W\beta)}{\partial\beta} + \frac{\partial(W\beta^*)}{\partial\beta^*} + (2\bar n + 1)\frac{\partial^2 W}{\partial\beta\partial\beta^*}\right) + \frac{\gamma_c}{2}\left(\frac{\partial(W\alpha)}{\partial\alpha} + \frac{\partial(W\alpha^*)}{\partial\alpha^*} + \frac{\partial^2 W}{\partial\alpha\partial\alpha^*}\right)\end{aligned} \tag{5}$$

As it stands this equation describes the full quantum behavior of the system and is equivalent to the master equation. Unfortunately, the presence of third-order derivative terms which arise from the non-linear optomechanical coupling significantly complicate the analysis as they mean that the equation is not of the Fokker–Planck type [30]. One way around this difficulty is to choose an alternative quasi-probability distribution, for which the resulting partial differential equation does not involve third-order derivatives such as the positive-P distribution [30,33]. Here, however, we take a simpler approach and simply neglect the third-order terms, an approach known as the *truncated Wigner approximation*. This amounts to a semiclassical approximation in which the zero-point noise in the cavity and resonator are correctly accounted for, but the non-linearity is not handled exactly. It is known from previous studies that the truncated Wigner function tends to work well when the fluctuations are weak, but it can fail quite badly in other regimes (for example it can get tunneling times

badly wrong in a bistable system) [30,33]. Thus provided we remain within the weak coupling regime where $g \ll 2\omega_m$ (which is where semiclassical approximations work best) we can expect that this simple approximation should at least capture the behavior of the resonator when it is in a well-defined limit-cycle in which the fluctuations in amplitude are small.

When the truncated Wigner function approximation is made, and the third-order derivative terms are dropped, the resulting equation of motion for the Wigner function is a standard Fokker–Planck equation from which we obtain the coupled Langevin equations [30],

$$\dot{\alpha} = i\left[\Delta + \frac{g}{2}\left(\beta + \beta^*\right)\right]\alpha - i\Omega - \frac{\gamma_c}{2}\alpha + \eta_\alpha \tag{6}$$

$$\dot{\beta} = i\frac{g}{2}\left(\alpha^*\alpha - \frac{1}{2}\right) - i\omega_m\beta - \frac{\gamma_m}{2}\beta + \eta_\beta \tag{7}$$

The noise terms have zero means and delta-correlated second moments,

$$\left\langle \eta_{\alpha^*}(t)\eta_\alpha\left(t'\right)\right\rangle = \delta\left(t - t'\right)\gamma_c/2 \tag{8}$$

$$\left\langle \eta_{\beta^*}(t)\eta_\beta\left(t'\right)\right\rangle = \delta\left(t - t'\right)\gamma_m\left(\bar{n} + \frac{1}{2}\right) \tag{9}$$

3. Resonator dynamics

Although we have already made an approximation to obtain a Fokker–Planck equation for the Wigner functions, the Langevin equations which result still describe a relatively complicated dynamics. To progress further we make use of the fact that the amplitude of the mechanical oscillations will change only slowly compared to the optical time-scales when both the optomechanical coupling and the mechanical damping are weak [22]. The idea is to exploit this separation of time-scales by solving the equation for α assuming a fixed *amplitude* for the mechanical oscillations, $|\beta|$, and then substituting the result into the equation for β to which the standard techniques of classical stochastic systems can then be applied.

We start by redefining the amplitude of the cavity, α, as a sum of an average and a fluctuating component,

$$\alpha = \langle\alpha\rangle + \delta\alpha \tag{10}$$

We will also assume that the cavity noise is weak so that the Langevin equation for the cavity amplitude can be written as

$$\dot{\beta} = i\frac{g}{2}\langle\alpha^*\rangle\langle\alpha\rangle - i\omega_m\beta - \frac{\gamma_m}{2}\beta + i\frac{g}{2}\left(\langle\alpha^*\rangle\delta\alpha + \langle\alpha\rangle\delta\alpha^*\right) + \eta_\beta \tag{11}$$

where the term $\delta\alpha^*\delta\alpha$ has been approximated by its average, $\langle\delta\alpha^*\delta\alpha\rangle = 1/2$.

We now use the assumption of a slowly changing resonator amplitude to define,

$$\beta = \beta_c + Be^{-i\phi}e^{-i\omega_m t} \tag{12}$$

where β_c is a constant shift in the origin of the resonator and the amplitude and phase B, ϕ are taken to be slowly varying functions of time. This form for β is substituted into the Langevin equation for α and we use the assumption of slowly evolving amplitude and phase to solve it neglecting the time dependence of B and ϕ. Working with the variables [22],

$$\tilde{\alpha} = \alpha e^{-iz\sin(\omega_m t+\phi)} \tag{13}$$

$$\tilde{\eta}_\alpha = \eta_\alpha e^{-iz\sin(\omega_m t+\phi)} \tag{14}$$

where $z = gB/\omega_m$ we find (after taking the Fourier transform),

$$\left\langle\tilde{\alpha}(\omega)\right\rangle = \frac{-i\Omega\sum_n \delta(\omega - \omega_m n)J_n(-z)e^{in\phi}}{\gamma_c/2 + i(\omega - \Delta')} \tag{15}$$

$$\delta\tilde{\alpha}(\omega) = \frac{\tilde{\eta}_\alpha(\omega)}{\gamma_c/2 + i(\omega - \Delta')} \tag{16}$$

where $\Delta' = \Delta + g\,\mathrm{Re}[\beta_c]$ and $J_n(z)$ is a Bessel function of the first kind of order n. We can now determine the corresponding resonator dynamics by substituting these expressions back into the equation of motion for β.

3.1. Back-action damping

We proceed by examining the first term which arises from the average dynamics of the cavity, $i\frac{g}{2}\langle\alpha^*\rangle\langle\alpha\rangle$. This term consists of a Fourier series with frequencies an integer multiple of ω_m (see Eq. (15)). Since we have assumed that the optomechanical coupling is weak, a rotating wave approximation can be made in which we drop all the terms in the

Fourier series except the constant one (which determines β_c) and the term oscillating at the mechanical frequency. Thus the center of the mechanical oscillations is found by equating non-oscillating terms,

$$\beta_c = \frac{g\Omega^2}{2\omega_m - i\gamma_m} \sum_n \frac{J_n^2(z)}{\gamma_c^2/4 + (\omega_m n - \Delta')^2} \tag{17}$$

Although this expression is non-linear, it can be evaluated to a good approximation by replacing Δ' with Δ in the denominator when the coupling is sufficiently weak.

The equation of motion for the oscillating part of the mechanical motion is then given by $\beta_r = \beta - \beta_c$,

$$\dot{\beta}_r = -i(\omega_m + \delta\omega)\beta_r - \frac{\gamma_m + \gamma_{BA}}{2}\beta_r + i\frac{g}{2}\left(\langle\alpha^*\rangle\delta\alpha + \langle\alpha\rangle\delta\alpha^*\right) + \eta_\beta \tag{18}$$

The terms coming from the average dynamics of the cavity lead to amplitude-dependent frequency shift and damping terms, which are defined as

$$\gamma_{BA}(z) = \frac{g^2\gamma_c\Omega^2}{2z} \sum_n \frac{J_n(z)J_{n+1}(z)}{|h_n h_{n+1}|^2} \tag{19}$$

$$\delta\omega(z) = -\frac{g^2\Omega^2}{2\omega_m z}\,\mathrm{Re}\left(\sum_n \frac{J_n(z)J_{n+1}(z)}{h_n h_{n+1}^*}\right) \tag{20}$$

where

$$h_n = \gamma_c/2 + i\left(\omega_m n + \Delta'\right) \tag{21}$$

The terms involving $\delta\alpha$ and $\delta\alpha^*$ in Eq. (18) are noise terms which arise from the fluctuations in the cavity (see Eq. (16)).

Much simpler expressions for the back-action damping and frequency shift can be derived if the system is well-within the resolved side-band regime ($\omega_m \gg \gamma_c$) and the system is tuned close to one of the resonances ($\delta = \Delta' - \omega_m p \ll \omega_m$ with p an integer),

$$\gamma_{BA}(z) = -\frac{\Omega^2\gamma_c}{[\gamma_c^2/4 + \delta^2]}\left(\frac{g}{\omega_m}\right)^2 \frac{p\,J_p^2(z)}{z^2} \tag{22}$$

$$\delta\omega(z) = -\frac{\Omega^2\delta}{[\gamma_c^2/4 + \delta^2]}\left(\frac{g}{\omega_m}\right)^2 \frac{J_p(z)}{z}\frac{\mathrm{d}J_p(z)}{\mathrm{d}z} \tag{23}$$

Knowledge of the back-action damping is already enough to provide a good picture of the average dynamics of the system, at least for weak enough couplings. In particular an analysis of the total damping $\gamma_m + \gamma_{BA}$ allows the different dynamical states of the system (and the associated bifurcations) to be identified [22].

3.2. Resonator probability distribution

The Langevin equation for the resonator amplitude (Eq. (18)) can be converted via a series of steps (described in Appendix A) into a Fokker–Planck equation for the energy $E = \beta_r\beta_r^*$. The steady-state solution of the Fokker–Planck equation is a probability distribution, $P(E)$, of the form

$$P(E) \propto \mathrm{e}^{-U(E)} \tag{24}$$

with an effective potential of the form

$$U(E) = \int_0^E \frac{\gamma_m + \gamma_{BA}(E')}{D_m + D_{BA}(E')}\,\mathrm{d}E' \tag{25}$$

The diffusion constants which arise from the effects of the thermal surroundings of the resonator (D_m) and the fluctuations in the cavity (D_{BA}) are given by

$$D_m = \gamma_m(\bar{n} + 1/2) \tag{26}$$

$$D_{BA}(E) = \frac{\gamma_c g^2\Omega^2}{8} \sum_n \frac{1}{|h_n|^2}\left|\frac{J_{n-1}(z)}{h_{n-1}} - \frac{J_{n+1}(z)}{h_{n+1}}\right|^2 \tag{27}$$

with $z = gE^{1/2}/\omega_m$. Note that we have neglected a small correction to the numerator in Eq. (25) arising from the noise terms, as discussed in Appendix A.

Although $P(E)$ is rather complex, considerable simplifications can be made in certain regimes as we describe in Section 5.2 below. For now we note that just as a simpler form for the back-action damping emerges when the system is close to a resonance ($\delta = \Delta' - \omega_m p \ll \omega_m$ with p an integer) and within the resolved side-band regime ($\omega_m \gg \gamma_c$), we can also obtain a simplified expression for D_{BA} valid in this regime,

$$D_{BA} = \frac{g^2\Omega^2}{8\omega_m^2}\frac{\gamma_c}{[\gamma_c^2/4+\delta^2]}\left\{2J_p^2(z) + \left[J_{p+1}(z) + J_{p-1}(z)\right]^2\right\} \tag{28}$$

4. Cooling regime

The theory of the resonator dynamics is well-understood in the regime where the laser drive is below the cavity frequency [8–11], $\Delta < 0$, so that energy tends to be transferred from the resonator to the cavity. In this regime the back-action damping is positive and the system is guaranteed to remain in a state where the mechanical oscillator simply fluctuates about a fixed point.

We can obtain a good approximation to the steady-state properties of the system (valid as usual for weak optomechanical coupling) in this limit by evaluating the back-action damping and diffusion in the limit where $z = gB/\omega_m \ll 1$. In this limit we can make use of the approximate expansions of the (integer order) Bessel functions,

$$J_n(z) \simeq \frac{1}{(n)!}\left(\frac{z}{2}\right)^n \tag{29}$$

for $n \geqslant 0$ (and note also $J_n(z) = J_{-n}(-z)$) and hence find,

$$\gamma_{BA} \simeq \gamma_{BA}^{(0)} = \frac{-\Delta' g^2\Omega^2\gamma_c\omega_m}{\gamma_c^2/4+\Delta'^2} \times \frac{1}{[\gamma_c^2/4+(\omega_m+\Delta')^2][\gamma_c^2/4+(\omega_m-\Delta')^2]} \tag{30}$$

where

$$\Delta' \simeq \Delta + \frac{g^2\omega_m\Omega^2/2}{(\gamma_m^2/4+\omega_m^2)(\gamma_c^2/4+\Delta^2)} \tag{31}$$

For $z \ll 1$ the back-action contribution to the diffusion takes the form,

$$D_{BA}^{(0)} = \frac{g^2\Omega^2\gamma_c}{(\gamma_c^2+4\Delta'^2)}\frac{(\gamma_c^2/4+\Delta'^2+\omega_m^2)}{[\gamma_c^2/4+(\Delta'+\omega_m)^2][\gamma_c^2/4+(\Delta'-\omega_m)^2]} \tag{32}$$

The steady-state solution for the energy probability distribution in this limit is

$$P(E) \propto \exp\left[\frac{-(\gamma_{BA}^{(0)}+\gamma_m)E}{\gamma_{BA}^{(0)}(n_{BA}+1/2)+\gamma_m(\bar{n}+1/2)}\right] \tag{33}$$

where we have defined

$$n_{BA} = \frac{\gamma_c^2+(\omega_m+\Delta')^2}{-4\Delta'\omega_m} \tag{34}$$

Finally, we recognize that the probability distribution, Eq. (33), is simply the Wigner function (after integrating out the phase) of an oscillator in a thermal state [30] with effective thermal occupation number,

$$n_{\text{eff}} = \frac{\gamma_{BA}^{(0)}n_{BA}+\gamma_m\bar{n}}{\gamma_{BA}^{(0)}+\gamma_m} \tag{35}$$

These results (Eqs. (30), (34) and (35)) of course match previous well-known calculations [8–11] based on linear response and linearization of the dynamics (about the cavity state). This is not surprising as in this regime the non-linearity due to the coupling between the optical and mechanical degrees of freedom does not play an important role and hence the truncated Wigner approximation should work well.

5. Limit-cycle dynamics

We now turn to consider the blue-detuned regime where the mechanical resonator is in effect pumped by the driven cavity. When the pumping of the resonator is strong enough to overcome the damping due to its surroundings it undergoes limit-cycle oscillations. In this regime the mechanical motion can lead to strong oscillations in the cavity occupation. Here we focus in particular on the fluctuations in the energy of the resonator within these limit-cycle states and use numerical methods to test the accuracy of our analytical approach.

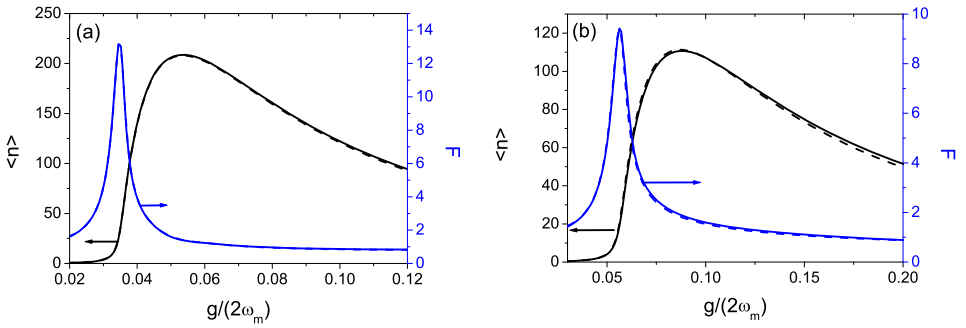

Fig. 1. Average occupation, $\langle n\rangle$ and Fano factor, F, of the cavity as a function of the coupling strength, g. (a) $\omega_m = \gamma_c$, $\Delta = 0.6$, $\Omega = 0.2$, $\bar{n} = 0$ and $\gamma_m = 1.6 \times 10^{-4}$. (b) $\Delta = \omega_m = 5$, $\Omega = 0.05$, $\bar{n} = 0$ and $\gamma_m = 3 \times 10^{-5}$. We adopt units where $\gamma_c = 1$. Numerical results are plotted with full lines and analytic results (which largely overlie the numerical ones) with dashed lines. In (a) F reaches a value of 0.83 for $g/(2\omega_m) = 0.12$ and in (b) F reaches a value of 0.85 for $g/(2\omega_m) = 0.2$.

5.1. Comparison of numerical and analytical calculations

The validity of the approximate analytic description of the resonator's state (Eq. (24)) can be checked, at least for a limited range of parameters, by comparing it with a numerical solution of the master equation, Eq. (2) (details of the method we use to obtain the steady-state density matrix of the system are given elsewhere, see for example Appendix A of Ref. [34]). The chief difficulty in obtaining a numerical solution is the number of states needed to describe the two oscillators which can be rather demanding of computer memory. Nevertheless, it is still possible to explore an interesting range of dynamical behaviors by choosing a relatively weak driving force for the cavity, together with an optomechanical coupling that is much stronger than the mechanical damping rate, $\gamma_c \gg \Omega \simeq g \gg \gamma_m$, whilst still remaining within the regime where we expect the truncated Wigner approach to be valid, $g \ll 2\omega_m$. Though this regime is rather different to that of most experiments where typically $g \ll \Omega$, significant progress towards stronger coupling strengths has been achieved in experiment [16,18] and the regime where $g \geqslant \Omega$ is attracting increasing interest from theorists [31,32,28].

A good picture of the resonator's dynamics as a function of parameters like the optomechanical coupling, g, and the detuning of the laser driving, Δ' (note we drop the prime on this quantity in what follows), is obtained from just the first two moments of $P(E)$. In comparing numerical and analytical results we need to recall that the $P(E)$ distribution is equivalent to a Wigner function (averaged over the phase) and hence the moments of this distribution correspond to symmetrically ordered operator averages [30] hence

$$\int_0^\infty E P(E)\,\mathrm{d}E = \langle n\rangle + 1/2 \tag{36}$$

$$\int_0^\infty E^2 P(E)\,\mathrm{d}E = \langle n^2\rangle + \langle n\rangle + 1/2 \tag{37}$$

where here $n = b^\dagger b$. Fig. 1 shows examples of how the average energy $\langle n\rangle$ and the Fano factor, $F = (\langle n^2\rangle - \langle n\rangle^2)/\langle n\rangle$ behave as the coupling is increased. In both cases we see very good agreement between the analytic and numerical calculations though differences between the two do become apparent for larger values of $g/(2\omega_m)$.

The parameters in Fig. 1(a) correspond to the case where the cavity decay rate and mechanical frequency are matched $\omega_m = \gamma_c$, which leads to a very strong interaction between the two sub-systems [27], while the parameters used in Fig. 1(b) correspond to the resolved side-band limit $\omega_m \gg \gamma_c$ where a strong transfer of energy occurs around $|\Delta| \simeq m\omega_m$, with m an integer. In both cases the dynamical transition from a state in which the resonator fluctuates about a fixed point to one in which limit-cycle oscillations occur is marked by a clear threshold in $\langle n\rangle$ and a corresponding peak appearing in the Fano factor. The transition is continuous in the sense that the size of the limit-cycle oscillations grows steadily from zero.

Although the distribution $P(E)$, and its first two moments in particular, give a fairly detailed picture of the resonator dynamics it is still helpful to look at the behavior of the system in the full phase space. Fig. 2 shows examples of the Wigner functions of the resonator calculated numerically for different values of the coupling strength for the parameters used in Fig. 1. For very weak couplings (Fig. 2(a)), the Wigner function appears as a small blob around the origin. As the coupling is increased this blob widens (Fig. 2(b)), an effect which is clearly seen as a dramatic increase in the Fano factor in Fig. 1(a). Then, beyond a certain coupling threshold, the density in the middle begins to drop so that a limit-cycle can be seen to form. Finally, for strong couplings the Wigner function takes the form of a narrow ring (Fig. 2(c)) corresponding to limit-cycle oscillations with a low level of amplitude fluctuations and hence a low value of F.

Looking at the highest values of $g/(2\omega_m)$ in Fig. 1 we see that a situation is reached where $F < 1$ corresponding to a number squeezing (a non-classical state) of the resonator [27,28]. However, it is important to note that reaching a regime

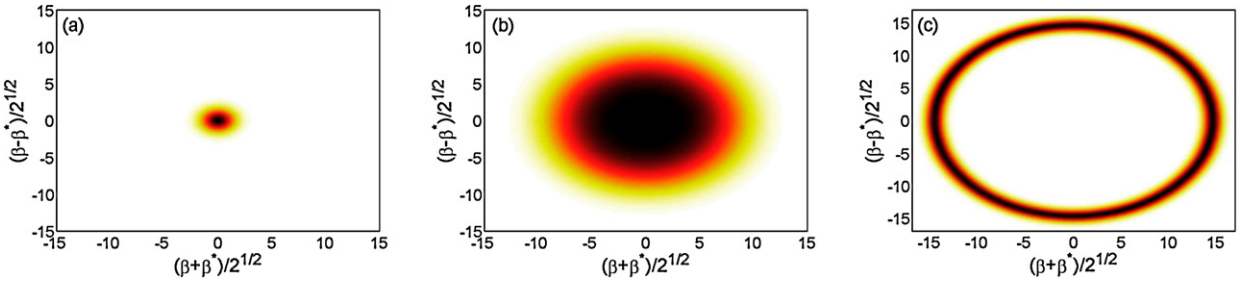

Fig. 2. Wigner functions of the resonator for (a) $g/(2\omega_m) = 0.02$ (below threshold), (b) $g/(2\omega_m) = 0.034$ (at threshold), (c) $g/(2\omega_m) = 0.11$ (above threshold). All other parameters are the same as in Fig. 1(a).

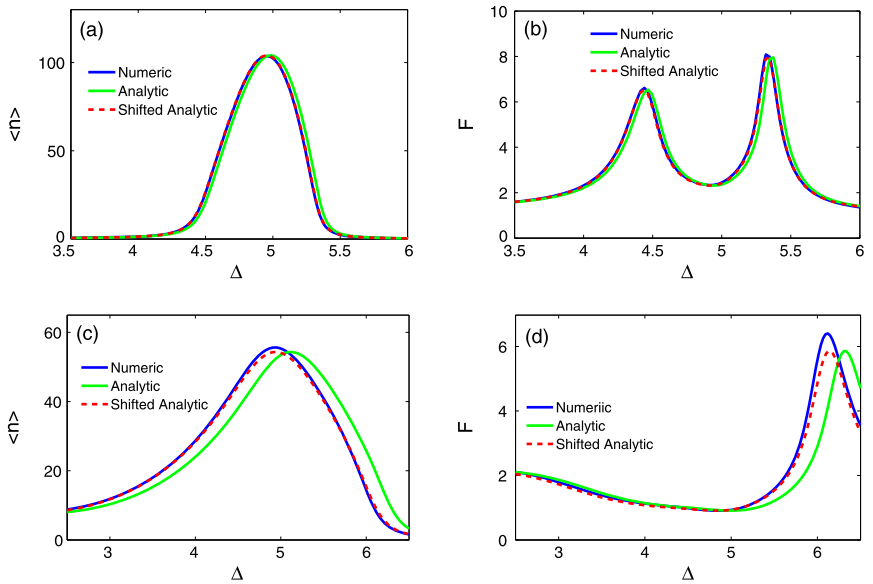

Fig. 3. Average occupation, $\langle n\rangle$ and Fano factor, F, of the cavity as a function of the detuning, Δ, for $\omega_m = 5$ and with coupling $g/(2\omega_m) = 0.075$ (a), (b); $g/(2\omega_m) = 0.19$ (c), (d). The other parameters are $\Omega = 0.05$, $\bar{n} = 0$ and $\gamma_m = 3 \times 10^{-5}$. Numerical results are plotted together with the analytic results. Also shown are curves of the analytic results shifted by plotting them as a function of $\tilde{\Delta} = \Delta - g^2/(4\omega_m)$ rather than Δ.

where $F < 1$ is strongly dependent on having almost no thermal noise in the system. In Fig. 1 the thermal occupation number, $\bar{n}$, is zero. A value of $\bar{n} \sim 1$ is sufficient to reach the regime where $F > 1$ for all the parameters studied here. The decrease in the Fano factor seen in Fig. 1 does not continue indefinitely with increasing coupling, but is in fact terminated by a transition to a different limit-cycle state. This transition is predicted by the analytic theory [22], but is not captured as accurately as the first (continuous) transition because of the rather large values of $g/(2\omega_m)$ involved and we will not explore this regime in any detail here.

It is interesting to compare the dynamics with that seen in quantum optical systems like the laser [30]. A continuous transition to a state of high-occupation is a hallmark of a laser. However, in a conventional laser there is a saturation in the average occupation at strong couplings and the Fano factor goes to unity (the photon statistics far above threshold are Poissonian as is the case for a coherent state). However, for our system, we see from Fig. 1 that as the coupling is increased beyond the dynamical transition, the Fano factor continues to drop and the average energy also declines. These features, although not seen in a conventional laser, are common in other laser-like systems where the coherent pumping of the oscillator has sufficiently low noise [35,30], such as the micromaser where the pumping arises from coherent coupling to just one other quantum system [36,37] (at any one time).

The agreement between the analytics and numerics in Fig. 1 appears to be very good, but a more nuanced picture is obtained by examining the behavior as a function of the detuning Δ. Fig. 3 compares the analytic predictions for $\langle n\rangle$ and F as a function of Δ for two different coupling strengths, $g/(2\omega_m) = 0.075$ and $g/(2\omega_m) = 0.19$, with parameters chosen to lie within the resolved side-band regime (matching those used in Fig. 1(b)). For the weaker coupling, $g/(2\omega_m) = 0.075$, the numerics and analytic curves agree well and we can see that the limit-cycle state (marked by a region of high $\langle n\rangle$ and relatively small F) is closely focussed on the resonance where $\omega_m = \Delta$. For the higher coupling, $g/(2\omega_m) = 0.19$, the region where $\langle n\rangle \gg 1$ is broader and we see that there is a distinct shift between the numerical and analytic results. In fact a simple renormalization of the cavity frequency so that $\tilde{\Delta} = \Delta - g^2/(4\omega_m)$ is enough to bring the analytic calculation back

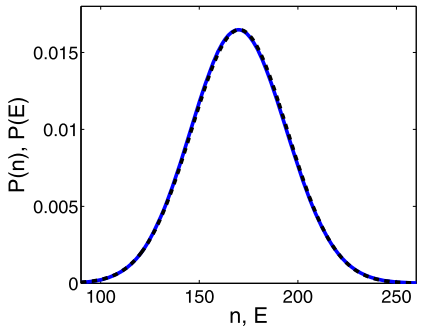

Fig. 4. Comparison of the probability distributions for the resonator obtained numerically, $P(n)$, with the Gaussian approximation of $P(E)$ calculated using Eq. (39). The numerical results (full curve) and the analytic calculation (dashed curve) follow one another very closely. Here $g/(2\omega_m) = 0.04$ and $\Delta = 0.75$. All other parameters are the same as in Fig. 1(a).

into good agreement with the numerics as is clear from the plots in Fig. 3. However, such a shift does not arise naturally within the semiclassical calculation we presented and must be added by hand. The fact that a shift like this occurs provides a strong hint that in this regime a better match might be obtained by using an approach that treats the cavity-resonator coupling exactly [31,32].

5.2. Gaussian description within a limit-cycle

When the system is well-within a limit-cycle we can approximate the $P(E)$ distribution as a Gaussian. The center of the limit-cycle, E_0, is given by the relationship $\gamma_{BA}(E_0) + \gamma_m = 0$ and assuming that the distribution is strongly peaked about this value we can expand the effective potential up to second order,

$$U(E) \simeq U(E_0) + \frac{(E-E_0)^2}{2}\frac{\mathrm{d}^2U(E)}{\mathrm{d}E^2}\bigg|_{E=E_0} \tag{38}$$

Thus we can write,

$$P(E) = \frac{1}{\sqrt{2\pi}\sigma_E}\mathrm{e}^{-(E-E_0)^2/2\sigma_E^2} \tag{39}$$

where

$$\sigma_E^2 = \frac{D_m + D_{BA}(E_0)}{\frac{\mathrm{d}\gamma_{BA}}{\mathrm{d}E}\big|_{E=E_0}} \tag{40}$$

These expressions can be simplified further using Eqs. (22) and (28) when the system is within the resolved side-band regime and tuned close to a resonance. This simple approximate form matches very well with numerical calculations of the number distribution of the resonator, $P(n) = \langle n|\hat{\rho}|n\rangle$, provided the system is well-within the limit-cycle regime and the optomechanical coupling is weak enough. Fig. 4 shows a comparison of the distributions calculated numerically and analytically (note that for $E_0, \sigma^2 \gg 1$ the distinctions between energy and number distributions (see e.g. Eqs. (36) and (37)) are insignificant and the two can be compared directly).

5.3. Amplitude noise suppression

Although a relatively modest level of thermal fluctuations ($\bar{n} \sim 1$) may be enough to destroy the number squeezing seen in Fig. 1, the energy fluctuations in the limit-cycle states are still interesting even in the presence of considerable thermal noise. Fig. 5 shows how the behavior of the average energy and Fano factor are affected by increasing $\bar{n}$. The region over which the transition into the high average energy state occurs is broadened, but for strong couplings the average energy is little changed. Note, however, the broadening of the $P(E)$ distribution which follows from adding significant thermal noise means that the non-linear character of the back-action damping and diffusion cannot be neglected and the distribution is no longer Gaussian (in fact a slight asymmetry emerges in $P(E)$). The energy fluctuations, measured by F, are clearly lower at high couplings (where the resonator is well-within the limit-cycle regime), than at $g = 0$.

The significance of the fluctuations in the energy of the resonator in the red-detuned regime were easy to understand as the system could be mapped onto a thermal state quantified by an effective occupation number. For the limit-cycle states in the blue-detuned regime, we can make a comparison with the behavior of a resonator coupled to the same thermal environment which is driven by a pure (i.e. noise free) harmonic drive instead of the cavity. In this case the drive does not add at all to the noise in the system, but the resonator is still affected by its thermal environment. Applying a pure

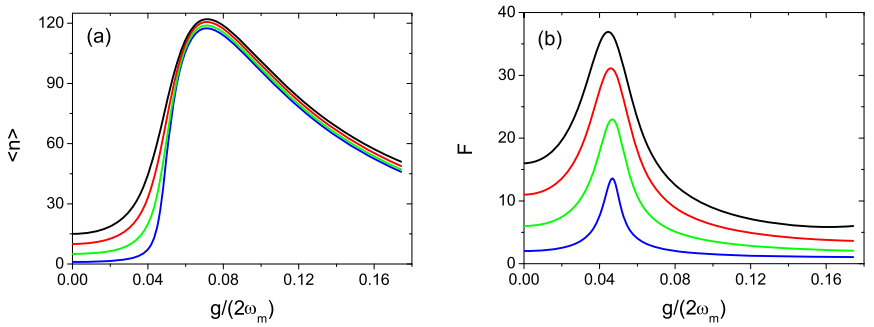

Fig. 5. Effect of thermal noise on limit-cycle dynamics. (a) Average occupation, $\langle n\rangle$ and (b) Fano factor, F, of the cavity as a function of the coupling strength, $g/(2\omega_m)$, with $\Delta = 0.6$ and $\omega_m = 1$. In each plot the curves are for (from top to bottom) $\bar{n} = 15, 10, 5, 1$. The other parameters are $\Omega = 0.15$, and $\gamma_m = 1.6 \times 10^{-4}$.

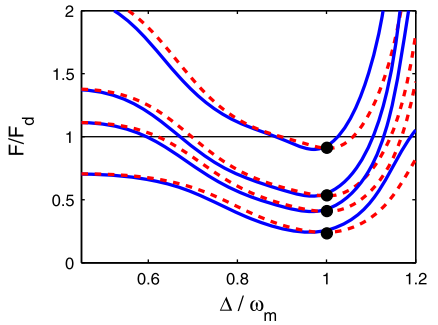

Fig. 6. Comparison of the Fano factor for the resonator within a cavity-driven limit-cycle state, F, with that of a displaced thermal state, F_d, chosen to have the same average energy, E_0 (see Eq. (42)) for $g/(2\omega_m) = 0.19$. From top to bottom the curves are for $\bar{n} = 0, 1, 2, 5$; the full curve comes from the numerics, the dashed line is obtained from the full analytical expression for $P(E)$ while the dots are from the approximate on-resonance expression, Eq. (44), evaluated at the first side-band resonance, $p = 1$. Parameters are the same as those used in Fig. 1(b).

harmonic drive to a state initially in a thermal state with occupation number $\bar{n}$, $\rho_{\rm th}(\bar{n})$, leads to a displaced thermal state [38] which is characterized by the finite amplitude ξ, and has the density operator,

$$\rho_{\rm DTS}(\xi, \bar{n}) = D(\xi)\rho_{\rm th}(\bar{n})D^{\dagger}(\xi) \tag{41}$$

where $D(\xi) = {\rm e}^{(\xi b^{\dagger} - \xi^* b)}$ is the displacement operator [30]. For a displaced thermal state with $E_0 = |\xi|^2$ the Fano factor is

$$F_d = \frac{[\bar{n}(1+\bar{n}) + (2\bar{n}+1)E_0]}{(\bar{n}+E_0)} \tag{42}$$

which reduces to unity for a zero temperature environment, $\bar{n} = 0$.

Close to the p-th side-band resonance in the good cavity limit (i.e. $(\Delta' - \omega_m p), \gamma_c \ll \omega_m$), we can find a simple expression for the energy fluctuations of the resonator. Well-within the limit-cycle regime, the resonator state is close to Gaussian (see Eq. (39)), and is well described by the parameters E_0 and σ_E. Provided that $E_0 \gg \sigma_E \gg 1$, we have

$$F \simeq \frac{\sigma_E^2}{E_0} = \frac{D_m + D_{BA}(E_0)}{E_0 \frac{{\rm d}\gamma_{BA}}{{\rm d}E}\big|_{E=E_0}} \tag{43}$$

Making use of the assumption that the system is close to resonance and in the good-cavity limit we can make use of Eqs. (22) and (28), together with the assumption that the resonator is in a stable limit-cycle so that $\gamma_m + \gamma_{BA}(E_0) = 0$, to obtain

$$F = \left[\left(p^2 + \frac{g^2 E_0}{2\omega_m^2}\right)\frac{1}{2p} + (\bar{n} + 0.5)\right] \times \left[\frac{J_p(z)}{J_p(z) - z\frac{{\rm d}J_p}{{\rm d}z}}\right]_{z = gE_0^{1/2}/\omega_m} \tag{44}$$

It is important to note that this formula will break down as soon as the coupling becomes strong enough for a second limit-cycle to become stable [27].

A comparison of the Fano factor for the resonator driven by the optical cavity with that of a displaced thermal state, chosen to have the same average energy, F_d, (see Eq. (42)) is shown in Fig. 6. We see that despite the slight effective shift in Δ which is apparent for this coupling strengths $g/(2\omega_m) = 0.19$, and is not captured in our theory, the approximate

on-resonance expression, Eq. (44) (with $p = 1$), works well. Even away from the center of the resonance, there is a clear suppression of the amplitude fluctuations when the resonator undergoes limit-cycle oscillations.

In essence the explanation for the low level of energy fluctuations in the limit-cycle regime is the same as that for the cooling which can be achieved with the same system for a different choice of laser detuning. Cooling is achieved when the fluctuations in the resonator (in this case about a stable fixed point in phase space) are strongly damped by the cavity which at the same time adds very little noise because the fluctuations in the number of photons in the cavity are very small (and set by fundamental quantum noise for $\hbar\omega_c \ll k_B T$). Within the limit-cycle regime, the resonator again fluctuates about a stable state (which in this case is a limit-cycle). Again it is the strong damping provided by the cavity combined with a very low level of fluctuations that allows the fluctuations in energy about the average of the limit-cycle to be rather low. In contrast, for a driven resonator in contact with a thermal environment the fluctuations about the average energy of the system are only damped by the same thermal environment for which the associated fluctuations are much higher (at a level of order $\bar{n} + 1/2$), as opposed to $1/2$ for the cavity (see Eqs. (9) and (8)). In a naive picture, the corresponding classical limit would mean no fluctuations at all in the cavity and hence an even lower level of energy fluctuations in the limit-cycles.

For either of the two dynamical states (fixed point or limit-cycle) energy fluctuations increase as one changes the parameters of the system towards a bifurcation, reducing the overall level of damping and making a given state less stable. A maximum in the level of fluctuations is seen as the system actually passes through a bifurcation and its state changes e.g. from a fixed point to a limit-cycle, an effect analogous to critical fluctuations in a phase transition (see Fig. 3). When the laser drive is blue-detuned, but the coupling is very weak so the system is still below threshold, the effect of the cavity is to *reduce* the damping of fluctuations about the fixed point which thus enhances the fluctuations, an effect often referred to as 'heating' [39]. However, as the coupling is increased and the system goes through a bifurcation one reaches a regime where the cavity reduces the fluctuations though in this case about a limit-cycle state.

6. Discussion and conclusions

We have used a truncated Wigner function approach to develop an approximate analytic description of a resonator parametrically coupled to an optical or microwave cavity mode. This provides a way of describing the resonator dynamics in the regime where the cavity is driven at a frequency above resonance where linearization methods fail. Comparison with numerical calculations shows that our approach works well for sufficiently weak optomechanical coupling. Interestingly, we find that the cavity-driven oscillations of the resonator are associated with rather low levels of fluctuations in the energy of the oscillator. In the limit of zero temperature the cavity can drive the resonator into a non-classical number-squeezed state whilst at finite temperature the energy fluctuations of the resonator can be strongly suppressed compared to those of a resonator at the same temperature which is driven by a pure harmonic drive.

In addition to the energy fluctuations, which we have considered in detail here, the resonator is also subject to phase diffusion when it is in a limit-cycle. It is this phase diffusion which, for example, ensures that in the limit-cycle regime the steady-state of the resonator Wigner function has the shape of a ring (see Fig. 2(c)) and determines the resonator's linewidth. The stochastic description of the resonator dynamics which emerges when the truncated Wigner approximation is made can easily be used to calculate the phase diffusion rate, as shown in Ref. [27], though we have not done so here.

The work discussed here points towards a number of interesting directions which could be pursued in the future. This paper has taken a rather theoretical point of view, focussing on the validity of truncated Wigner approximation and characterizing exactly how well the analytic approximations it leads to actually describe the dynamics. Exactly how one could probe the level of the energy fluctuations has not been addressed. The obvious place to look is in the spectral properties of the light leaking out of the cavity which should provide information about the time-scales of the resonator dynamics and the fluctuations in its energy (and phase) [28]. Another issue we have not explored is the behavior of the system in the limits of strong drive, but weak optomechanical coupling. Whilst a full numerical treatment of this regime (which is relevant to most current experiments) seems very challenging, we expect that the truncated Wigner function approach developed here should give a good description.

Finally, we have not looked in detail at the regime where the resonator dynamics is bistable. In this case one expects extremely slow fluctuations to take the system between very different dynamical states. Since the fluctuations in this regime cannot in any way be considered small, one might expect a dramatic failure of the truncated Wigner function approach, as has been found in other strongly non-linear systems [33].

Acknowledgements

This work was supported by EPSRC under Grants EP/E03442X/1 and EP/I017828/1.

Appendix A. Formulation and solution of Fokker–Planck equation

In this appendix we show how a Fokker–Planck equation is obtained from the Langevin equation for the mechanical amplitude (Eq. (18)) and demonstrate that the corresponding steady-state solution is given, to a good approximation, by Eq. (24). The calculation is rather involved because of the non-linearity of the noise terms arising from the cavity. Our

calculation follows Lax's approach, detailed in Refs. [40,29], which amounts to treating Eq. (18) using the Stratonovich rules [41].

Starting from the Langevin equation for β_r, Eq. (18), we switch to variables whose evolution is slow (compared to ω_m, γ_c). We introduce the quantities x and y, defined by the relation $x - iy = \beta_r e^{i\omega_m t} = \sqrt{E}e^{-i\phi}$, and write down corresponding equations of motion,

$$\dot{x} = -\frac{\gamma_T}{2}x - \delta\omega y + \frac{1}{2}\left(\eta_\beta e^{i\omega_m t} + \eta_{\beta^*} e^{-i\omega_m t}\right) - \sigma \sin(\omega_m t) \tag{45}$$

$$\dot{y} = -\frac{\gamma_T}{2}y + \delta\omega x + \frac{i}{2}\left(\eta_\beta e^{i\omega_m t} - \eta_{\beta^*} e^{-i\omega_m t}\right) - \sigma \cos(\omega_m t) \tag{46}$$

Here $\delta\omega$ is the back-action correction to the resonator frequency (defined in Eq. (20)), $\gamma_T = \gamma_m + \gamma_{BA}$ is the sum of the mechanical damping rate due to the resonator's thermalized surroundings and the back-action damping (defined in Eq. (19)), and we have defined the noise originating from fluctuations in the cavity as $\sigma = g(\langle\alpha^*\rangle\delta\alpha + \langle\alpha\rangle\delta\alpha^*)/2$. The back-action damping, frequency correction and the noise, σ, are all functions of the scaled mechanical amplitude $z = (g/\omega_m)\sqrt{x^2 + y^2}$.

The coupled Langevin equations (Eqs. (45) and (46)) can be used to calculate the drift and diffusion coefficients of the system from which a Fokker–Planck equation for the resonator can be formulated [41,40]. The calculation is complicated not just by the fact that the noise term arising from the cavity, σ, depends on the variables x and y but also because it is multiplied by an oscillating function. However, time-independent expressions for the drift and diffusion terms can be obtained by again exploiting the separation of time-scales in the system for weak optomechanical coupling which imply that x and y evolve only very slowly on times $\sim 1/\omega_m, 1/\gamma_c$ [29].

The drift coefficient for x is defined as

$$A_x = \frac{\langle \Delta x(t)\rangle}{\Delta t} \tag{47}$$

where Δt is a time increment which is in some sense small (as we discuss below) and $\Delta x = x(t + \Delta t) - x(t)$. The expression for A_y takes the same form. The diffusion coefficients are defined as

$$D_{xx} = \frac{\langle \Delta x^2(t)\rangle}{2\Delta t} \tag{48}$$

$$D_{xy} = \frac{\langle \Delta x(t)\Delta y(t)\rangle}{2\Delta t} \tag{49}$$

and there is again an analogous expression for D_{yy}. Using Eq. (45) we have

$$\Delta x(t) = -\left(\frac{\gamma_T}{2}x(t) + \delta\omega y(t)\right)\Delta t + \frac{1}{2}\int_t^{t+\Delta t} ds\left[\eta_\beta(s)e^{i\omega_m s} + \eta_{\beta^*}(s)e^{-i\omega_m s}\right] - \int_t^{t+\Delta t} ds\,\sigma(s)\sin(\omega_m s) \tag{50}$$

The time interval Δt is assumed to be long compared to $1/\gamma_c$ and $1/\omega_m$, but still small compared to the time-scale over which x and y change [29].

We require $\Delta x(t)$ in the expression for A_x accurate to order Δt, but for the diffusion terms such as D_{xx} we only require $\Delta x(t)^2$ to order Δt [40]. Thus for the diffusion terms it is sufficient to simply use the values of x and y at time t to evaluate $\sigma(s)$ in Eq. (50) and hence for D_{xx}, for example, we have

$$\begin{aligned} D_{xx} = {} & \frac{1}{8\Delta t}\int_t^{t+\Delta t} ds \int_t^{t+\Delta t} ds'\left[\left\langle\eta_\beta(s)\eta_{\beta^*}(s')\right\rangle e^{i\omega_m(s-s')} + \left\langle\eta_{\beta^*}(s)\eta_\beta(s')\right\rangle e^{-i\omega_m(s-s')}\right] \\ & + \frac{1}{2\Delta t}\int_t^{t+\Delta t} ds \int_t^{t+\Delta t} ds'\left\langle\sigma(s)\sigma(s')\right\rangle \sin(\omega_m s)\sin(\omega_m s') \end{aligned} \tag{51}$$

The first line of this expression is readily evaluated as the thermal noise is delta-correlated (Eq. (9)). In the second line, we neglect terms which oscillate as a function of t at frequencies $\sim \omega_m$ are neglected [29], leading to a coarse-grained diffusion constant which has no explicit time dependence (essentially the same result is achieved by simply averaging over a period [27]).

The drift terms require a higher level of approximation and hence for them we use

$$\sigma(s) = \sigma\left(x(t), y(t); s\right) + \left.\frac{d\sigma}{dx}\right|_{x=x(t)}\left(x(s) - x(t)\right) + \left.\frac{d\sigma}{dy}\right|_{y=y(t)}\left(y(s) - y(t)\right) \tag{52}$$

The small differences, e.g. $x(s) - x(t)$, are then evaluated using an expression similar to Eq. (50) which leads to terms involving a product of σ with one of its derivatives which do not average to zero. Thus we have

$$A_x = -\left(\frac{\gamma_T}{2}x(t) + \delta\omega y(t)\right) + \frac{1}{\Delta t}\int_t^{t+\Delta t} \mathrm{d}s \sin(\omega_m s)\int_t^s \mathrm{d}s' \left[\left\langle\left(\mathrm{d}\sigma(s)/\mathrm{d}x\right)\sigma(s')\right\rangle \sin(\omega_m s') + \left\langle\left(\mathrm{d}\sigma(s)/\mathrm{d}y\right)\sigma(s')\right\rangle \cos(\omega_m s')\right] \tag{53}$$

where here $\sigma(s) = \sigma(x(t), y(t); s)$, $\sigma(s') = \sigma(x(t), y(t); s')$ and terms which oscillate as a function of t are again neglected. Thus we see that the noise arising from the cavity leads to a contribution to the drift coefficient.

We now change to the energy and phase variables $E = x^2 + y^2$ and $\phi = \arctan(y/x)$ and obtain the associated drift and diffusion coefficients via the transformations [40]

$$D'_{ij} = \left(\frac{\partial a'_i}{\partial a_k}\right)\left(\frac{\partial a'_j}{\partial a_l}\right) D_{kl} \tag{54}$$

$$A'_i = \left(\frac{\partial a'_i}{\partial a_k}\right) A_k + \left(\frac{\partial^2 a'_i}{\partial a_m \partial a_n}\right) D_{mn} \tag{55}$$

with $a_1 = x$, $a_2 = y$ and $a'_1 = E$, $a'_2 = \phi$, and a repeated suffix implies a summation. With the drift and diffusion coefficients in hand we can write down the form of a Fokker–Planck equation for the probability distribution of the resonator. However, for our purposes it is enough to consider probability distributions which are a function of E only (as will be the case in the steady-state for a broad range of conditions) and to average over the phase. This leaves us with a Fokker–Planck equation for the energy probability distribution, $P(E)$, which takes the form,

$$\frac{\partial P(E)}{\partial t} = -\frac{\partial}{\partial E}\left[A_E P(E)\right] + \frac{\partial^2}{\partial E^2}\left[D_{EE} P(E)\right] \tag{56}$$

The corresponding stationary solution is

$$P(E) = N \exp\left\{\int_0^E \mathrm{d}E' \, \frac{A_E(E') - \frac{\mathrm{d}D_{EE}(E')}{\mathrm{d}E'}}{D_{EE}(E')}\right\} \tag{57}$$

where N is a normalization constant. The diffusion constant is given by

$$D_{EE} = E\left[D_m + D_{BA}(E)\right] \tag{58}$$

where $D_m = \gamma_m(\bar{n} + 1/2)$ and $D_{BA}(E)$ is defined in Eq. (27). Note that we can write $D_{EE} = E(D_0 + D_1)$, where

$$D_0 = D_m + f_{n,n}(\omega_m, z) + f_{n,n}(-\omega_m, z) \tag{59}$$

$$D_1 = -\left[f_{n,n-2}(\omega_m, z) + f_{n,n+2}(-\omega_m, z)\right] \tag{60}$$

with

$$f_{n,n'}(\omega, z) = \sum_n \left(\frac{g^2\Omega^2\gamma_c}{8h_n h^*_{n'}}\right) \frac{J_n(z) J_{n'}(z)}{[\gamma_c^2/4 + (\omega - \omega_m n - \Delta')^2]} \tag{61}$$

The drift term, A_E, is

$$A_E = -\gamma_T E + \frac{E}{2}\frac{\mathrm{d}D_{BA}}{\mathrm{d}E} + D_0 + \alpha_\phi \tag{62}$$

where

$$\alpha_\phi = \left(\frac{g\Omega}{2}\right)^2 \sum_n \frac{n J_n^2(z)\gamma_c}{\gamma_c^2 + 4(\Delta' + \omega_m n)^2}\left[\frac{1}{\gamma_c^2/4 + [(n+1)\omega_m + \Delta']^2} - \frac{1}{\gamma_c^2/4 + [(n-1)\omega_m + \Delta']^2}\right] - \left(\frac{g\Omega}{2}\right)^2 \sum_n J_n(z) J_{n+2}(z) \times \mathrm{Re}\left[\frac{1}{(\gamma_c/2 + i[\omega_m n + \Delta'])(\gamma_c/2 - i[\omega_m(n+2) + \Delta'])(\gamma_c/2 + i[\omega_m(n+1) + \Delta'])}\right] \tag{63}$$

The numerator in the potential term in the expression for $P(E)$ (Eq. (57)) is given by

$$\begin{aligned} A_E - \frac{\mathrm{d}D_{EE}}{\mathrm{d}E} &= -(\gamma_m + \gamma_{BA})E - D_1 - \frac{E}{2}\frac{\mathrm{d}D_{BA}}{\mathrm{d}E} + \alpha_\phi \\ &= -(\gamma_m + \gamma_{BA} + \delta\gamma_{BA})E \end{aligned} \tag{64}$$

with the correction to the back-action damping coming from the noise terms defined as

$$\delta\gamma_{BA} = \frac{1}{2}\frac{\mathrm{d}D_{BA}}{\mathrm{d}E} + \frac{D_1 - \alpha_\phi}{E} \tag{65}$$

Note that in the main body of the paper we have neglected $\delta\gamma_{BA}$. We have checked numerically that $\delta\gamma_{BA}$ is indeed a small correction for the parameters used here, but is also possible to see why this is so more generally. In the limit of small z (the limit relevant for the cooling regime), an expansion of the relevant Bessel functions shows that $\delta\gamma_{BA}$ may safely be dropped as the z-independent term has an extra factor of $(g/\omega_m)^2$ compared to the one arising in γ_{BA}. In the limit-cycle regime, where E is large, neglecting $\delta\gamma_{BA}$ can again be justified, in this case both g/ω_m and $1/E$ are small quantities.

References

[1] T.J. Kippenberg, K.J. Vahala, Science 321 (2008) 1172.
[2] I. Favero, K. Karrai, Nature Photon. 3 (2009) 201.
[3] F. Marquardt, S.M. Girvin, Physics 2 (40) (2009).
[4] S. Bose, K. Jacobs, P.L. Knight, Phys. Rev. A 59 (1999) 3204.
[5] M. Aspelmeyer, K. Schwab (Eds.), Focus on Mechanical Systems at the Quantum Limit, New J. Phys. 10 (2008) 095001.
[6] M. Poot, H.S.J. van der Zant, Phys. Rep. 511 (2012) 273.
[7] O. Arcizet, P.-F. Cohadon, T. Briant, M. Pinard, A. Heidmann, J.-M. Mackowski, C. Michel, L. Pinard, O. Français, L. Rousseau, Phys. Rev. Lett. 97 (2006) 133601.
[8] I. Wilson-Rae, N. Nooshi, W. Zwerger, T.J. Kippenberg, Phys. Rev. Lett. 99 (2007) 093901.
[9] F. Marquardt, J.P. Chen, A.A. Clerk, S.M. Girvin, Phys. Rev. Lett. 99 (2007) 093902.
[10] M.P. Blencowe, E. Buks, Phys. Rev. B 76 (2007) 014511.
[11] C. Genes, D. Vitali, P. Tombesi, S. Gigan, M. Aspelmeyer, Phys. Rev. A 77 (2008) 033804.
[12] O. Arcizet, P.-F. Cohadon, T. Briant, M. Pinard, A. Heidmann, Nature 444 (2006) 71.
[13] J.D. Thompson, B.M. Zwickl, A.M. Jayich, F. Marquardt, S.M. Girvin, J.G.E. Harris, Nature 452 (2008) 72.
[14] A. Schliesser, A. Schliesser, O. Arcizet, R. Rivière, G. Anetsberger, T.J. Kippenberg, Nature Phys. 5 (2009) 509.
[15] S. Gröblacher, J.B. Hertzberg, M.R. Vanner, G.D. Cole, S. Gigan, K.C. Schwab, M. Aspelmeyer, Nature Phys. 5 (2009) 485.
[16] J. Chan, T.P. Mayer Alegre, A.H. Safavi-Naeini, J.T. Hill, A. Krause, S. Gröblacher, M. Aspelmeyer, O. Painter, Nature 478 (2011) 89.
[17] T. Rocheleau, T. Ndukum, C. Macklin, J.B. Hertzberg, A.A. Clerk, K.C. Schwab, Nature 463 (2010) 72.
[18] J.D. Teufel, T. Donner, D. Li, J.W. Harlow, M.S. Allman, K. Cicak, A.J. Sirois, J.D. Whittaker, K.W. Lehnert, R.W. Simmonds, Nature 475 (2011) 359.
[19] T. Carmon, H. Rokhsari, L. Yang, T.J. Kippenberg, K.J. Vahala, Phys. Rev. Lett. 94 (2005) 223902.
[20] C. Metzger, M. Ludwig, C. Neuenhahn, A. Ortlieb, I. Favero, K. Karrai, F. Marquardt, Phys. Rev. Lett. 101 (2008) 133903.
[21] G. Anetsberger, O. Arcizet, Q.P. Unterreithmeier, R. Rivière, A. Schliesser, E.M. Weig, J.P. Kotthaus, T.J. Kippenberg, Nature Phys. 5 (2009) 909.
[22] F. Marquardt, J.G.E. Harris, S.M. Girvin, Phys. Rev. Lett. 96 (2006) 103901.
[23] S. Zaitsev, A.K. Pandey, O. Shtempluck, E. Buks, Phys. Rev. E 84 (2011) 046605.
[24] S. Zaitsev, O. Gottlieb, E. Buks, arXiv:1104.2235, 2011.
[25] M. Ludwig, B. Kubala, F. Marquardt, New J. Phys. 10 (2008) 095013.
[26] K.J. Vahala, Phys. Rev. A 78 (2008) 023832.
[27] D.A. Rodrigues, A.D. Armour, Phys. Rev. Lett. 104 (2010) 053601.
[28] J. Qian, A.A. Clerk, K. Hammerer, F. Marquardt, arXiv:1112.6200.
[29] M. Lax, Phys. Rev. 160 (1967) 290.
[30] D.F. Walls, G.J. Milburn, Quantum Optics, Springer-Verlag, Berlin, 1994.
[31] P. Rabl, Phys. Rev. Lett. 107 (2011) 063601.
[32] A. Nunnenkamp, K. Børkje, S.M. Girvin, Phys. Rev. Lett. 107 (2011) 063602.
[33] P. Kinsler, P.D. Drummond, Phys. Rev. A 43 (1991) 6194.
[34] T.J. Harvey, D.A. Rodrigues, A.D. Armour, Phys. Rev. B 78 (2008) 024513.
[35] M.A.M. Marte, P. Zoller, Phys. Rev. A 40 (1986) 5774.
[36] D.A. Rodrigues, J. Imbers, A.D. Armour, Phys. Rev. Lett. 98 (2007) 067204.
[37] H. Walther, B.T.H. Varcoe, B.-G. Englert, T. Becker, Rep. Prog. Phys. 69 (2006) 1325.
[38] H. Saito, H. Hyuga, J. Phys. Soc. Jpn. 65 (1996) 1648.
[39] See for example, O. Arcizet, P.-F. Cohadon, M. Pinard, A. Heidmann, Nature 444 (2006) 71.
[40] M. Lax, Rev. Mod. Phys. 38 (1966) 541.
[41] H. Risken, The Fokker–Planck Equation, 2nd ed., Springer-Verlag, Berlin, Germany, 1989.